



## Effects of adsorption properties of particle electrodes on the degradation of acid red 14 using three-dimensional electrode system

Feizhen Li, Di Xie, Yuan Zhao, Lijun Liu, Wenyan Liang\*

Beijing Key Lab for Source Control Technology of Water Pollution, College of Environmental Science and Engineering, Beijing Forestry University, Beijing 100083, China, Tel. +86 13661243958; Fax: +86 10 62336615; email: lwy@bjfu.edu.cn (W. Liang), Tel. +86 13020027246; email: lifeizhen2013@163.com (F. Li), Tel. +86 13120124636; email: xieditust@126.com (D. Xie), Tel. +86 15201444285; email: liulijunmail@163.com (L. Liu), Tel. +86 18810121662; email: zhaoyuan\_809027@126.com (Y. Zhao)

Received 10 May 2016; Accepted 18 February 2017

### ABSTRACT

Four types of granular activated carbon (GAC), i.e., two coal-based activated carbon ( $\phi=4$  mm, CBAC-4;  $\phi=1.5$  mm, CBAC-1.5), coconut shell activated carbon (CSAC), and nut shell activated carbon (NSAC), were selected to investigate the effects of their adsorption properties on the degradation of acid red 14 (AR-14) by using three-dimensional electrode system. The results of Brunauer–Emmett–Teller surface area analysis, scanning electron microscopy, and Fourier transform infrared spectroscopy indicated that obvious differences in the surface morphologies, textural properties, and surface functional groups among them were not observed. Based on the pseudo-second-order and Freundlich model, the adsorption velocity and capacity followed the order: NSAC > CSAC  $\approx$  CBAC-4 > CBAC-1.5. According to the variation of AR-14, chemical oxygen demand, and total organic carbon concentrations in the electro-oxidation processes, the order of the four GACs on AR-14 degradation and removal was approximately NSAC > CSAC > CBAC-4  $\approx$  CBAC-1.5. The increase in hydraulic retention time was more beneficial to GACs with higher adsorption property. The GACs with lower adsorption property required higher current and energy consumption to obtain the similar efficiency for AR-14 removal. Thus, the particle electrodes should be the material with good adsorption capacity toward the target pollutants.

*Keywords:* Adsorption property; Particle electrode; Granular activated carbon; Electro-chemical oxidation; Acid red 14

### 1. Introduction

Electro-chemical oxidation is frequently applied in biorefractory wastewater treatment due to its prominent advantages such as high efficiency, simple operation, and environmental friendliness [1]. It is often realized through a two-dimensional (2D) electrode system, which is composed of couples of anodes and cathodes [2]. The rate of electro-chemical reaction is dependent on electron transfer rate attributed to the heterogeneous electron transfer between the solid electrode and the substrate in the solution. Further,

this rate is directly proportional to the specific surface area of the electrode [3]. However, enhancement of the surface area cannot be achieved in a conventional 2D electrode system.

The three-dimensional (3D) electrode technology, which involves the addition of particle electrodes between the anode and cathode, has been attracting significant attention due to the extensive specific surface area in comparison with 2D electrodes [4]. Under the influence of an electric field at an appropriate voltage, the particles can be polarized, which leads to the formation of charged microelectrodes [5]. Therefore, the distance between the substrate and the particle electrodes can be shortened, and the mass transfer can be increased significantly [3]. The extensive specific surface

\* Corresponding author.

area of the particle electrodes provides more reactive sites to the substrate, resulting in higher electrolytic efficiency [6]. Numerous studies have shown that the 3D electrode behaves more efficiently for organic degradation compared with the 2D electrode under the same experimental conditions [4,7–9].

Hitherto, the technology of 3D electrode has been successfully applied for the elimination of organic pollutants, such as methyl orange [10], C.I. acid orange 7 [3], polyacrylamide [11], paper mill wastewater [12], petroleum refinery wastewater [9], anionic surfactants [4], heavy oil refinery wastewater [7], reactive brilliant red X-3B [13], phenols [14], rhodamine B [15], and citric acid [16]. The studies revealed that the behavior of 3D electrode system was affected by the electrode materials (anode, cathode, and particle electrode), reactor structure, current/voltage, pH values, temperature, and initial concentration of pollutants [3]. Among these factors, particle electrodes play a fundamental role in estimating the performance of the entire system. Till now, particle electrodes frequently used in electro-chemical oxidation are dominantly carbonaceous and metallic (including metal oxide) materials, including granular activated carbon (GAC) [3,5,10–12,14], carbon aerogel [13], porous ceramsite [7,17], alumina [18], MnOx–NiOy–PO<sub>4</sub><sup>3-</sup> modified kaolin [4], molecule sieve [19], zeolite [20], iron particle [9], foam nickel particle [6], and steel slag [15]. Selection of appropriate electrode material is a critical factor during the design and operation of 3D electro-chemical oxidation reactor. However, selection of appropriate particles electrodes has not been clearly described in most of the studies. Lv et al. [34] compared the removal efficiency of phenol from wastewater using GAC, commercial carbon particle electrode, and carbon aerogel particles. They found that the carbon aerogel achieved the greatest degradation efficiency on phenol simulated wastewater and indicated that the best performance was attributed to the numerous mesopores and micropores and regular structure of the carbon aerogel. Although kaolin is a non-conductive material, it was also selected to prepare the particle electrodes due to its adsorption ability for anionic surfactants. Interestingly, they achieved more than 86% removal of surfactant [4]. Li et al. [35] employed GAC as particle electrodes for ammonia degradation by 3D electrodes, attributed to good ammonia adsorption capability of GAC. It is obvious that the most particle electrodes can also be used as the adsorbents to remove the pollutants present in water or for wastewater treatment [21,22]. Adsorption or electro-sorption ability in the 3D electro-chemical oxidation is also considered as one of the main characteristics of particles electrodes [23]. Till date, extensive research efforts have been devoted to the effects of particle electrodes on the pollutant removal; however, the influences of adsorption properties of particle electrodes on the pollutant degradation have rarely been investigated.

Carbon-based particle electrode, in particular, the activated carbon, has been most commonly used in the 3D electrode technology; therefore, four types of GACs were selected as the particle electrodes to investigate the effects of adsorption properties on the electro-oxidation. Acid red 14 (AR-14) was selected as a model azo dye because of its spread use in variety of industries and stable characteristics with respect to biochemical oxidation. The surface morphology, textural properties, and surface functional groups of the

GACs were characterized. Four simplified models, including pseudo-first-order and pseudo-second-order equations, and the Langmuir and Freundlich equations were used to describe the adsorption kinetics and isotherm. The common factors influencing the 3D electro-oxidation, namely hydraulic retention time (HRT), current, and initial pH, were investigated to understand their effects on GACs with different adsorption properties.

## 2. Materials and methods

### 2.1. Dye material

AR-14 (C<sub>20</sub>H<sub>12</sub>N<sub>2</sub>Na<sub>2</sub>O<sub>7</sub>S<sub>2</sub>, ≥99%) was obtained from Beijing Qianmen Chemical Raw Material Co., Ltd., China. It was used as received without further purification.

### 2.2. Granular activated carbon

Four types of GACs were purchased from Beijing Kecheng Guanghua Co., Ltd., China, namely two types of coal-based activated carbon (φ = 4 mm, CBAC-4 and φ = 1.5 mm, CBAC-1.5), coconut shell activated carbon (CSAC; φ = 0.8–2 mm), and nut shell activated carbon (NSAC; φ = 0.8–2 mm). All the GACs were washed several times using distilled water to remove the impurities and dried at 100°C prior to the experiments.

### 2.3. Adsorption kinetics and isotherm

AR-14 solution (200 mg/L) was prepared using distilled water without pH adjustment. In the evaluation of adsorption kinetics, GAC (1.000 g) was added to AR-14 solution (250 mL). The mixture was stirred at 150 rpm at 25°C for 40 h in a thermostatic shaker. At specified time intervals, the AR-14 concentration of the supernatant was measured. In the tests of adsorption isotherms, GAC (1.000 g) was mixed with AR-14 solution (100 mL) with different concentrations. Then, the mixture was also stirred at 150 rpm and 25°C. The AR-14 concentration of the supernatant was measured after 20 h. The AR-14 adsorption capacity at equilibrium was calculated by using Eq. (1):

$$q_e = \frac{(C_0 - C_e)V}{m} \quad (1)$$

where  $q_e$  is the amount of AR-14 adsorbed at equilibrium (mg/g);  $C_0$  and  $C_e$  are the initial and equilibrium concentrations of AR-14 (mg/L), respectively;  $m$  is the dry mass of GAC (g); and  $V$  is the volume of the solution (L).

### 2.4. Experimental setup

The 3D electrode apparatus was composed of a tank, a pump, a rectangular cell, an anode electrode, a cathode electrode, particle electrodes, and a direct current power source (Fig. 1). The specification of cell was  $L \times W \times H = 60 \text{ mm} \times 50 \text{ mm} \times 120 \text{ mm}$ . The cathode and anode were titanium mesh (Ti, 50 × 120 mm) and titanium mesh coated with ruthenium (IV) oxide (Ti/RuO<sub>2</sub>, 50 × 120 mm), respectively. The distance between the two electrodes

was 60 mm. The GAC was filled between the two electrodes with the height of 70 mm and volume of  $\sim 200 \text{ cm}^3$ . A support layer was attached to the cell and was used to load up with active carbon particles near the bottom.

### 2.5. Experimental procedure

The simulated wastewater was prepared by dissolving AR-14 in sodium sulfate solution ( $\text{Na}_2\text{SO}_4$ , 0.03 mol/L) at the concentration of 200 mg/L without pH adjustment unless otherwise stated. The experiments were performed under continuous upflow mode without circulation by using peristaltic pump. Before electrolysis, the GAC in the reactor was pretreated by continuously feeding AR-14 wastewater from the influent tank at the flow rate of 10 mL/min for 20 min, thus minimizing the effect of the GAC adsorption on the AR-14 removal. During electrolysis, the effluent was sampled at different intervals to detect the AR-14 concentration, chemical oxygen demand (COD), total organic carbon (TOC), and ultraviolet–visible (UV–Vis) spectra.

In order to probe the behavior of four types of GACs, the current density and HRT were set at a specific value of 0.6 A and 20 min, respectively. Different HRT in the 3D electrode bed were achieved by adjusting the flow rate, where the current was set at 0.1 and 0.6 A, and flow rate was varied from 10 to 16 mL/min, i.e., HRT 20–12 min. To explore the effects of current, HRT was remained at 20 min; however, the current was changed from 0.1 to 0.6 A. The effect of pH was studied by adjusting the pH of dye solutions using 0.1 M HCl and NaOH solutions.

### 2.6. Analytical methods

The concentrations of AR-14 were measured using a UV–Vis spectrophotometer (T6, Persee Apparatus, China) at 504 nm. The decolorization rate was calculated according to Eq. (2) as follows:

$$\% \text{ decolorization} = \frac{C_0 - C}{C_0} \quad (2)$$

where  $C_0$  and  $C$  are AR-14 concentrations before and after electrolysis, respectively.

The COD and TOC were determined using a COD analyzer (CTL-12, Chengde Huatong Environmental

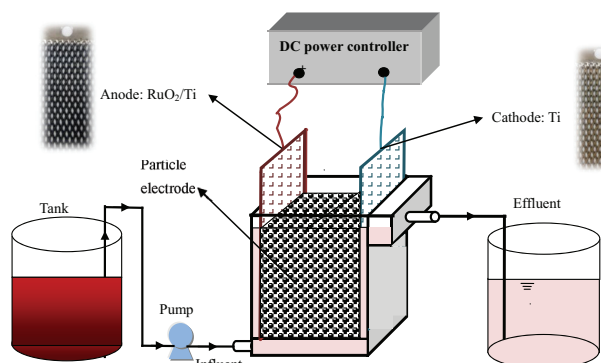


Fig. 1. Schematic of reaction system used in the experiments.

Protection Apparatus, China) and a TOC analyzer (TOC-V CSN, Rigaku, Japan), respectively. The UV–Vis absorption spectra were obtained from 190 to 750 nm using a spectrophotometer (UV-2600, Techcomp., China).

The surface properties of GAC were analyzed by scanning electron microscopy using a microscope (S-3400N, Hitachi, Japan) operated at 5 kV. The functional groups on GAC surface were identified by Fourier transform infrared spectrometer (VERTEX70, Bruker, Germany) and quantified by Boehm titration [24]. Specific surface area and pore volume were detected using pore analyzer (ASAP2020, Micromeritics, USA) and calculated by using the Brunauer–Emmett–Teller (BET) equation and Barrett–Joyner–Halenda algorithm, respectively.

## 3. Results and discussion

### 3.1. The surface properties of GAC

Similar surface morphologies of the CBAC-4 and CBAC-1.5 were observed in Fig. 2, with rough and uneven surface with relatively irregular distribution of holes on the surfaces. The surface of CSAC was relatively flat, and the pore distribution was more regular. However, a large number of circular macropores were distributed on the surface of NSAC. Although the four GACs exhibited different morphologies, their textural properties were similar as listed in Table 1. The BET surface area and pore volume of CSAC and NSAC were only slightly higher than those of CBAC-4 and CBAC-1.5. According to the pore size distribution, the pores of four GACs mainly consisted of micropores ( $< 2 \text{ nm}$ ). The adsorption of small molecule compounds on GAC is often attributed to the presence of micropores [21]. However, presence of mesopores (2–50 nm) not only leads to the adsorption of the

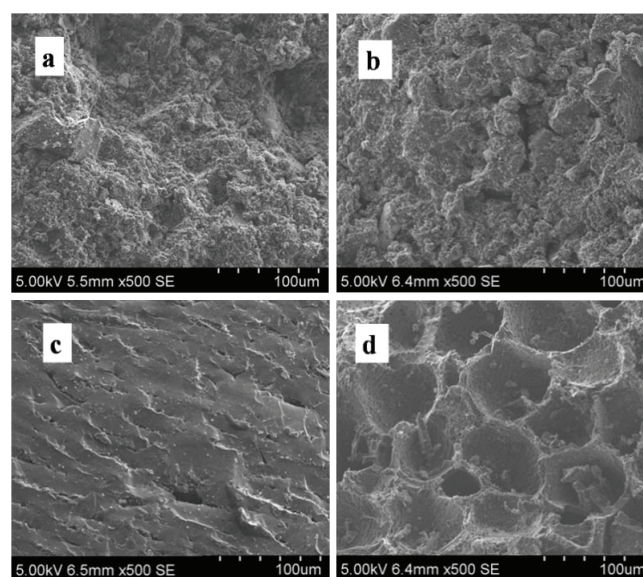


Fig. 2. Scanning electron microscopy images of the granular activated carbon: (a) coal-based activated carbon ( $\phi = 4 \text{ mm}$ , CBAC-4); (b) coal-based activated carbon ( $\phi = 1.5 \text{ mm}$ , CBAC-1.5); (c) coconut shell activated carbon (CSAC); and (d) Nut shell activated carbon (NSAC).

larger molecules but also increases the performance to act as potential candidates in other applications, such as catalytic carrier and electric double layer capacitors [25].

The functional groups of the four GACs (Fig. 3(a)) also exhibit similar infrared spectroscopic features, i.e., a very broad band corresponding to hydroxyl and carboxyl vibration from 3,600 to 3,200  $\text{cm}^{-1}$ , carbonyl vibration at 1,615–1,710  $\text{cm}^{-1}$ , phenolic hydroxyl vibration at 1,000–1,100  $\text{cm}^{-1}$ , and C–H or C–C stretching absorption around 600  $\text{cm}^{-1}$  [26]. The sharp peak at 1,384  $\text{cm}^{-1}$  shows a very strong intensity, and it could be attributed to carboxyl and ester groups [26]. Thus, the carboxyl, carbonyl, anhydrides, phenol, quinone, and lactone groups were identified on carbon surfaces. Further, several major functional groups were quantified (Fig. 3(b)). The results revealed that CBAC-4 and NSAC owned more functional groups than other two GACs, and CBAC-4 possessed the most contents of basic and carboxyl groups. Conventional GAC is synthesized by physical or chemical activation of organic precursors, such as coal, wood, fruit shell, or polymers, at elevated temperatures [25]. The GAC contains alkaline oxides if it is activated in high temperature steam; however, acidic oxides are formed on surface with zinc chloride activation [26]. The four GACs used in this study were produced in the same manufacturing plant; therefore, the same activation process made them have the similar textural properties and functional groups.

### 3.2. Adsorption kinetics and isotherm of GAC

A kinetic study was performed and presented in Fig. 4(a). A majority of AR-14 adsorption equilibrium was accomplished in 20 h for all the four GACs and remained stable after 24 h. This showed that the adsorption of AR-14 on GAC exhibited the characteristics involving rapid adsorption but slow balancing. The adsorption kinetic data were fitted with two kinetic models: pseudo-first-order and pseudo-second-order models. The equations are rearranged as Eqs. (3) and (4):

$$\ln(q_e - q_t) = \ln q_e - K_1 \left( \frac{t}{2.303} \right) \quad (3)$$

$$\frac{t}{q_i} = \frac{1}{(K_2 q_e^2)} + \frac{t}{q_e} \quad (4)$$

where  $q_e$  (mg/g) is the amount of AR-14 adsorbed at equilibrium;  $q_t$  (mg/g) is the amount of AR-14 adsorbed at time  $t$  (h);  $K_1$  ( $\text{h}^{-1}$ );  $K_2$  ( $\text{g}/\text{mg}\cdot\text{h}$ ) are rate constants of respective Eqs. (3) and (4). The pseudo-second-order kinetics

(Table 2) provided the better fitting for all the experimental data with  $R^2 > 0.97$ , indicating that the overall rate of the AR-14 adsorption process should be controlled by the pore diffusion in accordance with the pseudo-second-order reaction mechanism. The plots (Fig. 4(a)) are not linear over the entire time range, indicating that more than one process affected the AR-14 adsorption. They can be explained in terms of a few processes, such as boundary layer diffusion and the intraparticle diffusion [27]. The intraparticle diffusion is likely to occur in two stages: the adsorbate molecule enters rapidly into macropores and wider mesopores, and then penetrates more slowly into smaller mesopores [28,29]. The intraparticle diffusion of AR-14 molecules into small mesopores is the rate-limiting step in the adsorption process. The value of  $q_e$  in pseudo-second-order model was proportional to the

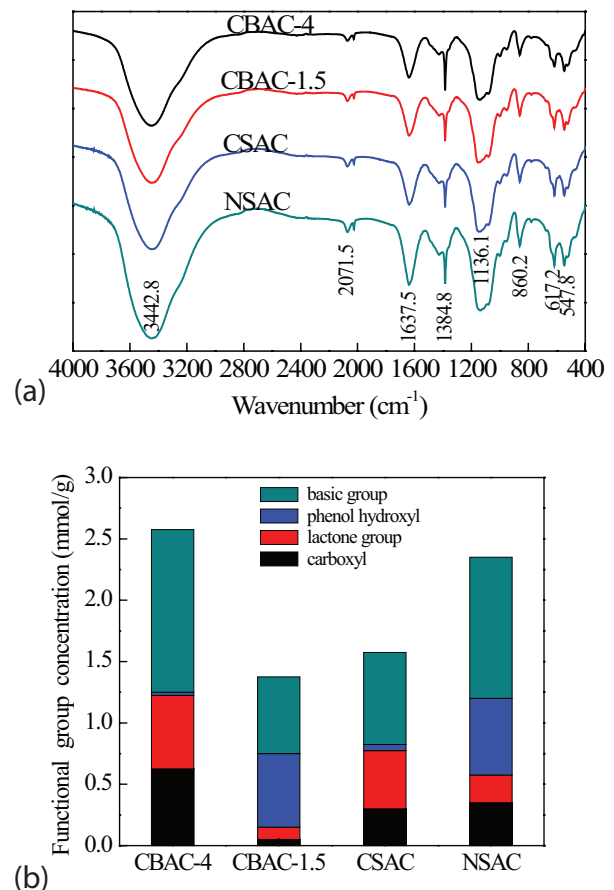


Fig. 3. The infrared spectra (a) and contents of functional groups (b) of the granular activated carbons.

Table 1  
The textural parameters of the granular activated carbons

	BET surface area ( $\text{m}^2/\text{g}$ )	$V_{\text{total}}$ ( $\text{cm}^3/\text{g}$ )	$V_{\text{micropore}}$ ( $\text{cm}^3/\text{g}$ )	Average pore size (nm)
Coal-based activated carbon ( $\phi = 4$ mm, CBAC-4)	835.5	0.794	0.619	3.804
Coal-based activated carbon ( $\phi = 1.5$ mm, CBAC-1.5)	703.5	0.815	0.611	4.632
Coconut shell activated carbon (CSAC)	1,146.5	1.047	0.921	3.652
Nut shell activated carbon (NSAC)	968.9	1.082	0.931	4.468

adsorption capacity; however,  $K_2$  was inversely proportional to the adsorption velocity. The NSAC obtained the greatest adsorption capacity at equilibrium. Moreover, the adsorption velocity roughly followed the order: NSAC > CSAC ≈ CBAC-4 > CBAC-1.5.

The Langmuir and Freundlich models were used to simulate the isotherm data in this study (Fig. 4(b)). The Langmuir isotherm assumed that the uptake of ion occurs on a homogenous surface by monolayer sorption limiting the adsorption due to the surface saturation; however, the Freundlich isotherm assumed that the uptake of ion occurs on a heterogeneous surface by multilayer adsorption [30]. Multilayer adsorption referred to the phenomenon of adsorption on the adsorbed molecules, and adsorption capacity increased with the size of the adsorption layer from inside to outside and gradually decreased [21]. The models can be expressed in the forms of Eqs. (5) and (6):

$$\frac{C_e}{q_e} = \frac{C_e}{q_m} + \frac{1}{Kq_m} \tag{5}$$

$$q_e = K_F C_e^{1/n} \tag{6}$$

where  $C_e$  (mg/L) is the equilibrium concentration;  $q_e$  (mg/g) is the amount adsorbed at equilibrium;  $q_m$  (mg/g) and  $K$  (L/mg) are the Langmuir constants;  $K_F$  ((mg/g) (g/L)<sup>n</sup>) and  $n$  are the Freundlich constants. The parameters listed in Table 2 indicate that the uptake of dye molecules by the four GACs initially increases sharply with increasing initial concentration and slowly approaches saturation. The equilibrium data fitted better to the Freundlich model than Langmuir model for all the GACs, indicating that the adsorption of AR-14 occurred on the heterogeneous surface by multilayer adsorption. The values of  $n$  and  $K_F$  in Freundlich model are related to the adsorbent–adsorbate affinity and the adsorption capacity, respectively [28]. The smaller values of  $n$  provide rapid adsorption processes. Therefore, the smallest value of  $n$  of NSAC indicated its best performance on adsorption capacity.

### 3.3. Degradation of acid red 14 by four types of GACs

The variation of concentrations of AR-14 in the electro-oxidation process were presented in Fig. 5(a). When NSAC was used as the particle electrode, the concentration of AR-14 in the effluent decreased from 175.2 to 5.94 mg/L after 20 min, which corresponded to nearly 97% decolorization. However, for the other three types of GACs, the concentrations of

AR-14 were maintained at 40–60 mg/L in the effluent, with the decolorization of 65%–77%.

The decolorization is usually considered as the first step in the degradation of azo dyes by electro-oxidation because of the damage of the chromophoric groups [5]. Then the by-products obtained during the decolorization are further degraded into inorganic substances, which can be expressed in terms of the variation of COD and TOC [1]. The similar variation tendency is also observed for the COD concentrations (Fig. 5(b)). NSAC still performed the best among the four types of GACs toward COD removal. After 20 min of treatment, the COD concentrations decreased from

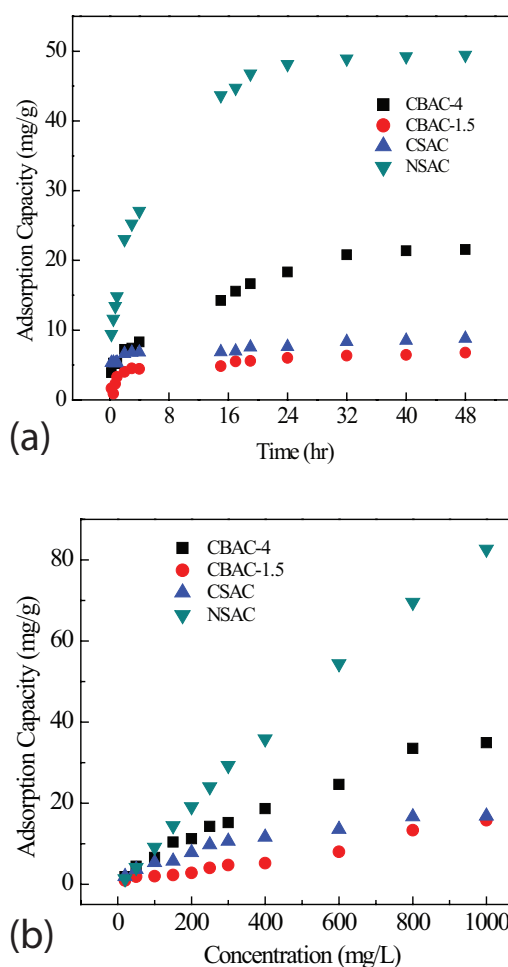


Fig. 4. Adsorption kinetics (a) and adsorption isotherm (b) profiles of the granular activated carbons.

Table 2  
The parameters of adsorption kinetics and isotherms

	Pseudo-first order			Pseudo-second order			Langmuir			Freundlich		
	$q_e$	$K_1$	$R^2$	$q_e$	$K_2$	$R^2$	$q_m$	$K_1$	$R^2$	$n$	$K_F$	$R^2$
CBAC-4	18.86	0.17	0.828	4.95	0.18	0.974	58.82	0.0014	0.888	1.33	0.514	0.983
CBAC-1.5	5.71	0.61	0.862	2.90	0.81	0.989	30.20	0.0008	0.361	1.44	0.365	0.951
CSAC	8.56	0.25	0.843	6.90	0.18	0.991	21.28	0.0033	0.966	1.78	0.662	0.982
NSAC	46.84	0.30	0.939	20.83	0.12	0.998	1,000	0.0001	0.258	1.02	0.367	0.997

135.4 to 22.7 mg/L, and continued to decrease to 2.2 mg/L after 60 min. Then, the COD concentration stabilized in the range 2.2–5.1 mg/L, corresponding to more than 96% removal. For the two CBACs, the removal efficiency of COD reached only the level of 30% after 100 min, the lowest among the GACs. After 180 min of treatment, the TOC concentrations shown in Fig. 5(c) reflect that the lowest TOC concentration of 10.5 mg/L is achieved in NSAC electro-oxidation, realizing 77% of mineralization. According to the variation of AR-14, COD, and TOC concentrations, the order of the four GACs for AR-14 degradation and removal was approximately NSAC > CSAC > CBAC-4 ≈ CBAC-1.5, which was similar to their adsorption property.

The UV–Vis spectra of the effluents after 180 min treatment were exhibited in Fig. 5(d). When AR-14 was dissolved in distilled water, three obvious absorption peaks could be seen between 200 and 600 nm. One peak, observed at 325 nm, was attributed to the benzene ring in dye molecules. Another peak, at 504 nm, was assigned to the azo structure of dye [31]. The peaks at 504 and 325 nm almost disappeared in NSAC electro-oxidation; however, they still existed in other three types of GACs' profiles. Further, the peaks at 229 nm decreased sharply in NSAC electro-oxidation; however, they only dropped slightly in other GACs' electro-oxidation processes. The degradation process of azo dyes during electro-oxidation often proceeds in three irreversible

steps: first, azo dyes are oxidized into the form of quinones; then quinones are oxidized into aliphatics by open-loop reactions; and finally aliphatics are mineralized into CO<sub>2</sub> and H<sub>2</sub>O [10]. Quinone material as an intermediate product exhibits characteristic absorption peaks at 226–230 nm, which matches with the peak shown in UV–Vis spectra. The disappearance of peak at 229 nm reflects the destruction of benzene ring in electro-oxidation processes. Compared with other GACs, NSAC can realize the open-loop reactions of AR-14 more efficiently, which leads to the highest effects of mineralization of the intermediates.

It is well known that the removal of pollutants in electro-oxidation processes consists of two aspects: the direct oxidation and indirect oxidation [32]. Direct oxidation, also called anode oxidation, refers to the direct oxidation of pollutants by the acceptance of electrons on the anode surface. It often takes place in two steps: (1) diffusion of pollutants from the bulk solution to the anode surface and (2) oxidation of pollutants at the anode surface [1]. The efficiency of the electro-oxidation depends on the relationship between mass transfer of the substrate and electron transfer at the electrode surface [33]. Although the existence of particle electrodes significantly enhances the contact areas between the substrate and electrodes, the rate of mass and electron transfer are different. The rate of electron transfer is determined by the electrode activity and current density; therefore, the rate of

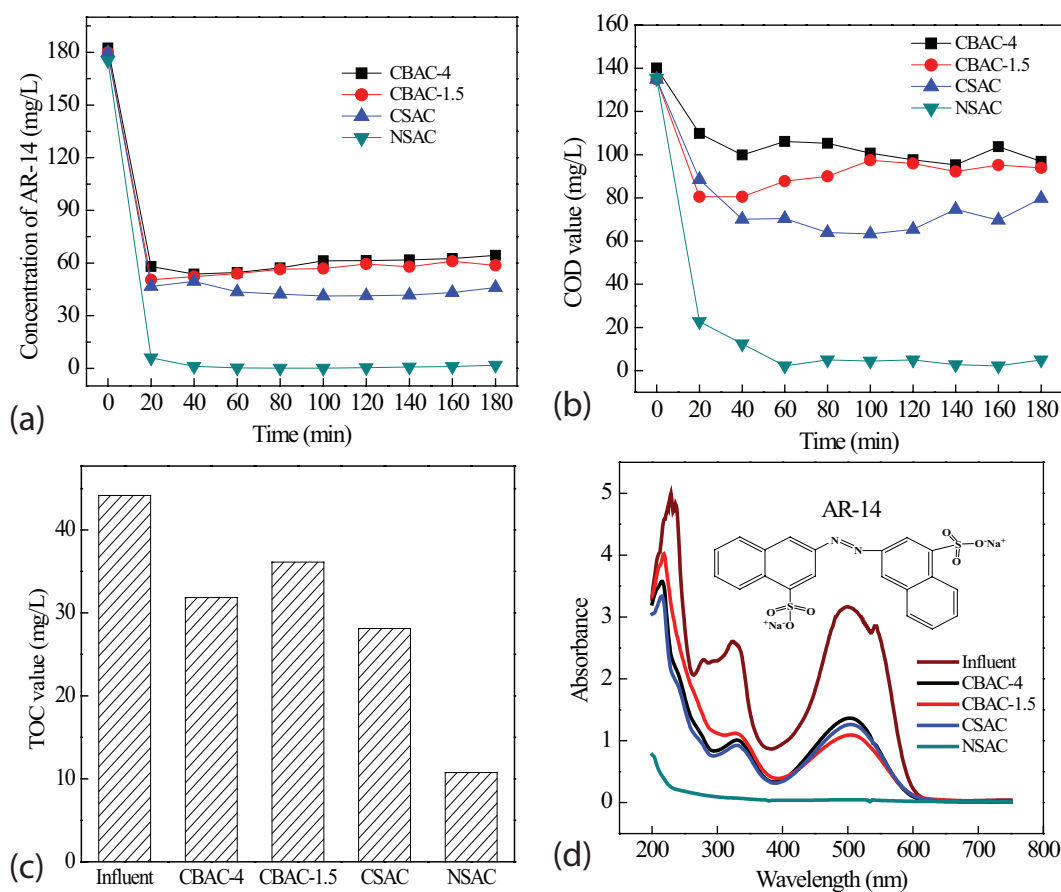


Fig. 5. The variation of AR-14 concentrations (a), chemical oxygen demand (b), total organic carbon (c), and UV–Vis spectra (d) in the three-dimensional electro-oxidation processes (current = 0.6 A; hydraulic retention time (HRT) = 20 min).

entire electro-oxidation process depends on the mass transfer if current density is high enough. The particles, which possess higher adsorption velocity and adsorption capacity, lead to rapid movement of the pollutant to the particle surface, which finally results in the accumulation of more amount of pollutants on the surface. Thus, NSAC behaved the best among the four GACs, even though the four GACs had the similar BET surface area.

The indirect oxidation is considered to be more important than the direct oxidation in the electro-chemical oxidation process. During the indirect oxidation, the pollutants are oxidized by the electro-generated oxidants such as hydroxyl radicals, active chlorine, hydrogen peroxide, ozone, and peroxodisulfuric acid [32]. The 3D electrode can generate more hydroxyl radicals than 2D electrode system due to the formation of microelectrodes under applied high potential [3,34]. The hydroxyl radicals electro-generated by the water electrolysis (Eq. (7)) are adsorbed on the surface of particle electrodes or diffuse near the particle electrodes, leading to the oxidation of organics and removal of COD (Eq. (8)) [17]. Thus, adsorption of more organics on the particle surface provides them with more chance to be oxidized. The particles that have significant adsorption of target pollutants, also behave well in indirect oxidation, which is another reason of NSAC's best performance. It reveals that the BET surface area of particle electrodes is not the decisive factor in the 3D electrode system; however, the adsorption character of the particle electrodes is more important in their degradation.



### 3.4. Effects of hydraulic retention time

HRT is an important factor in bed column adsorption studies due to its intensive influence on the contact time between adsorbent and adsorbate [28,29]. In order to investigate the effects of HRT on particle electrodes with different adsorption capacity, NSAC and CBAC-4 were selected, and the results are presented in Fig. 6.

In the test groups of current 0.1 A (Fig. 6(a)), there was no difference between NSAC and CBAC-4 at the HRT of 12 min, in which the AR-14 concentrations decreased to 138.1–139.9 mg/L in the effluent. When the HRT increased to 20 min, both the GACs had an obvious increment of degradation efficiency. However, the NSAC could reduce the AR-14 concentrations to 63.2 mg/L, much lower than 119.3 mg/L in CBAC-4 electro-oxidation. Further, the improvement in decolorization efficiency was also observed with the increase in HRT at current 0.6 A (Fig. 6(b)) similar to that of 0.1 A. It was obvious that the higher HRT favored the degradation of AR-14, regardless of the type of GAC and the magnitude of current. However, higher HRT could improve the effects of GACs with greater adsorption capacity more efficiently.

In general adsorption bed, the high HRT is conducive to the adsorption, and the low HRT is unfavorable [28,29]. In the 3D electrode system, the HRT also affects the contact time

between pollutants and particle electrodes, and then aids in determining the retention time of the pollutants adsorbed on the particle electrodes. The effects of electro-oxidation process depend on the rate of adsorption because the oxidation usually occurs rapidly [32]. When the HRT increased from 12 to 20 min, NSAC could adsorb more amount of AR-14 than CBAC-4 due to better adsorption properties of NSAC, which resulted in the greater removal efficiency. Similar results were also observed during ammonia removal using zeolite as particle electrodes [35]. The effects of HRT also reveal that the adsorption properties of particle electrode play a critical role in 3D electrode system. Moreover, HRT exhibits greater impact on materials with higher adsorption capability than those with lower adsorption.

### 3.5. Effects of current

In order to study the effects of current on particle electrodes with different adsorption capacity, NSAC and CBAC-4 were also selected, and the results are presented in Fig. 7. When the current is increased from 0.1 to 0.6 A, the concentration of AR-14 in the effluent decreases from 138.1 to 64.4 mg/L in NSAC electro-oxidation, and from 60.2 to 1.9 mg/L in

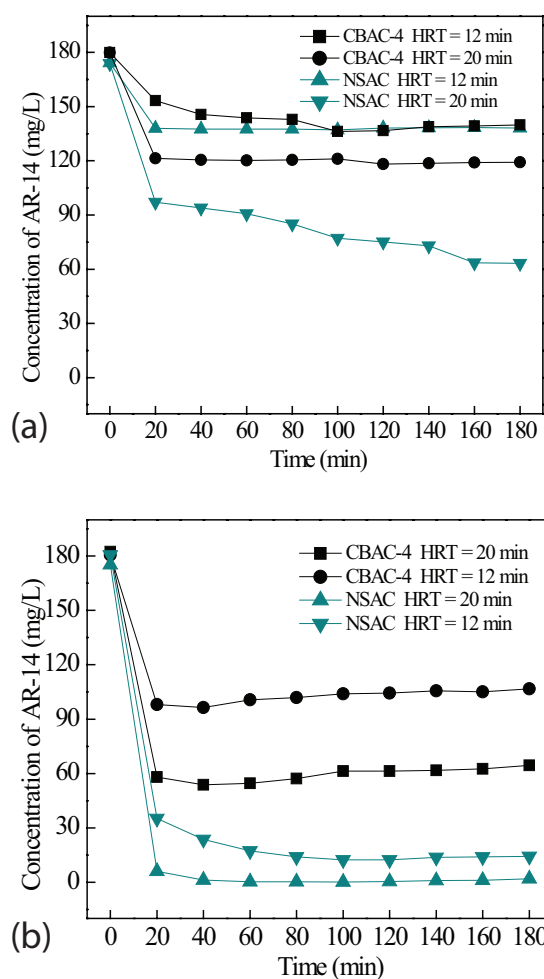


Fig. 6. The effects of HRT on the degradation of AR-14 at the current 0.1 A (a) and 0.6 A (b).

CBAC-4 electro-oxidation. The degradation of AR-14 was better as the current increased either in NSAC or in CBAC-4 electro-oxidation process. In most researches, the current exhibits obvious positive relationship with pollutant removal efficiency because it influences not only the electro-chemical oxidation but also the polarization behavior of particle electrodes [1,36]. The increase in current density was found to enhance the oxidant production, leading to high rate of pollutant removal through direct oxidation [1]. Furthermore, the increase in the applied current can improve the production of more electro-generated oxidants [10]. Thus, the number of electrons on particle electrodes that increases along with the current are essential for the oxidation processes and might lead to a superior performance [32]. Although NSAC and CBAC-4 exhibited different adsorption capacity toward AR-14, they were able to achieve better operation at elevated current.

However, the degradation of AR-14 in CBAC-4 electro-oxidation is far behind its degradation in NSAC electro-oxidation (Fig. 7). The AR-14 in effluent was 64.4 mg/L at current of 0.6 A in CBAC-4 electro-oxidation, only slightly higher than 60.2 mg/L at current of 0.1 A in NSAC electro-oxidation; however, significantly higher than 17.2 mg/L at current of 0.3 A in NSAC electro-oxidation. This indicates that the CBAC-4 consumes more amount of electricity than NSAC to obtain the same efficiency. Thus, for the particle electrodes with weak adsorption capacity, the higher current can remedy a defect of their lower efficiency. If the current is high enough, the gap between the particles with different adsorption capacity is shortened.

### 3.6. Effects of initial pH

We also investigated the influence of initial pH on the degradation of AR-14 using NSAC and CBAC-4 particle electrodes (Fig. 8). The initial pH does not influence the degradation of AR-14, irrespective of the type of GACs used. The major difference between the two GACs was that the overall effects of NSAC were higher than those of CBAC-4. This phenomenon was different from that mentioned in most of other studies related to 3D electrode system, in which the acidic environment is more beneficial to remove the pollutants than neutral or basic environment [4,11]. The pH of AR-14 influent was not buffered in this study; therefore, it could be changed during the treatment. No matter how the initial pH values changed, the pH of the effluents was kept stable in neutral condition, i.e., 7.1–7.3, even after 10 min treatment. This is another phenomenon that was observed to be different compared with other studies, in which the pH of effluent is often acidic [17]. When the influent gushed into the electrode bed, the water electrolysis resulted in the production of  $H^+$  and  $OH^-$  ions that might neutralize the alkalinity or acidity of influent. This made the pH of AR-14 solution to be neutral in the electrode bed, and thus the initial pH did not affect the degradation of AR-14.

The initial pH is a crucial parameter that plays an important role in the electro-oxidation treatment, because it influences the form of the electro-generated active species and its oxidation potential [11,12]. The acidic environment is more beneficial to produce free radical such as  $\bullet OH$  [11]. Therefore, a significant COD reduction can be obtained at a

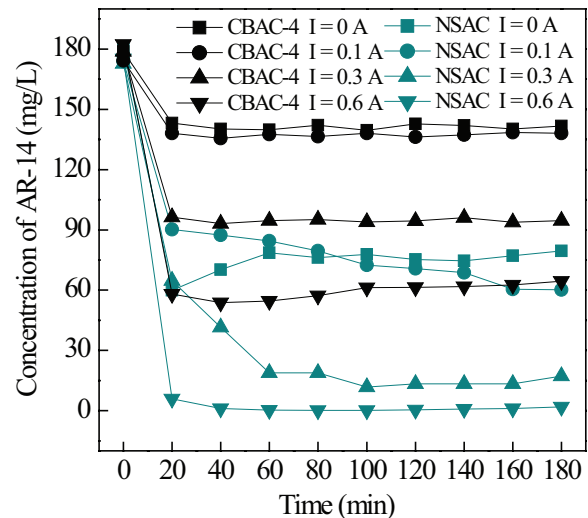


Fig. 7. Variation of AR-14 concentration with different currents (HRT = 20 min).

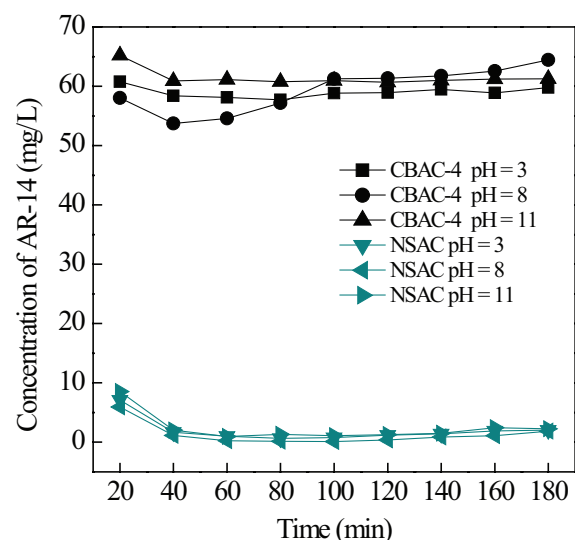


Fig. 8. The effects of initial pH on AR-14 degradation (current = 0.6 A; HRT = 20 min).

relatively low initial pH; however, a less COD reduction is observed in basic solution [9,11]. Even if the modified kaolin, which was not an electric conductive material, was used as 3D electrode, the optimal pH was 3, and 3D electrodes worked more efficiently at a lower pH [4]. At higher pH, more hardness would be removed, largely via  $CaCO_3$  or  $CaMgCO_3$  precipitation [16]. However, the carbonate and bicarbonate, the final oxidized products of organics at high pH, are two well-known  $\bullet OH$  radical scavengers [14]. The effects of initial pH on particle electrodes with different adsorption property were not obvious due to the neutral environment of electrode bed in this study.

## 4. Conclusions

The present study showed that the adsorption properties of particle electrodes significantly influenced the effects of

3D electrode system. The particle electrodes with higher adsorption capacity and velocity were favorable to the degradation, removal, and mineralization of organic pollutants. NSAC exhibited the best performance toward the degradation of AR-14 due to the best adsorption property among the four types of GACs used in this study. The HRT had greater impact on GAC with higher adsorption capacity than those with lower adsorption capacity. The increase in the applied current could improve the removal efficiency of AR-14, irrespective of the type of GACs applied; however, the GACs with lower adsorption capacity consumed more energy to obtain the same removal efficiency. The initial pH did not influence the GACs with different adsorption capacity in this study. The results indicated that the material with good adsorption properties for the target pollutants should be selected as particle electrode in 3D electrode system.

### Acknowledgments

This work was supported by Major Science and Technology Program for Water Pollution Control and Treatment of China (2013ZX07209001-003 and 2012ZX07307-001-006) and the Fundamental Research Funds for the Chinese Central Universities (2015ZCQ-HJ-02).

### References

- [1] G.H. Chen, Electrochemical technologies in wastewater treatment, *Sep. Purif. Technol.*, 38 (2004) 11–41.
- [2] D. Woisetschlager, B. Humpl, M. Koncar, M. Siebenhofer, Electrochemical oxidation of wastewater – opportunities and drawbacks, *Water Sci. Technol.*, 68 (2013) 1173–1179.
- [3] L. Xu, H. Zhao, S. Shi, G. Zhang, J. Ni, Electrolytic treatment of C.I. Acid Orange 7 in aqueous solution using a three-dimensional electrode reactor, *Dyes Pigm.*, 77 (2008) 158–164.
- [4] W.P. Kong, B. Wang, H.Z. Ma, L. Gu, Electrochemical treatment of anionic surfactants in synthetic wastewater with three-dimensional electrodes, *J. Hazard. Mater.*, 137 (2006) 1532–1537.
- [5] H.Z. Zhao, Y. Sun, L.N. Xu, J.R. Ni, Removal of Acid Orange 7 in simulated wastewater using a three-dimensional electrode reactor: removal mechanisms and dye degradation pathway, *Chemosphere*, 78 (2010) 46–51.
- [6] W. Liu, Z.H. Ai, L.Z. Zhang, Design of a neutral three-dimensional electro-Fenton system with foam nickel as particle electrodes for wastewater treatment, *J. Hazard. Mater.*, 243 (2012) 257–264.
- [7] L.Y. Wei, S.H. Guo, G.X. Yan, C.M. Chen, X.Y. Jiang, Electrochemical pretreatment of heavy oil refinery wastewater using a three-dimensional electrode reactor, *Electrochim. Acta*, 55 (2010) 8615–8620.
- [8] M.H. Zhou, L.C. Lei, The role of activated carbon on the removal of *p*-nitrophenol in an integrated three-phase electrochemical reactor, *Chemosphere*, 65 (2006) 1197–1203.
- [9] L. Yan, H.Z. Ma, B. Wang, Y.F. Wang, Y.S. Chen, Electrochemical treatment of petroleum refinery wastewater with three-dimensional multi-phase electrode, *Desalination*, 276 (2011) 397–402.
- [10] P. He, L. Wang, J. Xue, Z. Cao, Electrolytic treatment of methyl orange in aqueous solution using three-dimensional electrode reactor coupling ultrasonics, *Environ. Technol.*, 31 (2010) 417–422.
- [11] Z.H. Kang, H.K. Li, Y.H. Xu, L. Chen, Electrolytic degradation of polyacrylamide in aqueous solution using a three-dimensional electrode reactor, *Desal. Wat. Treat.*, 51 (2013) 2687–2694.
- [12] B. Wang, W. Kong, H. Ma, Electrochemical treatment of paper mill wastewater using three-dimensional electrodes with Ti/Co/SnO<sub>2</sub>-Sb<sub>2</sub>O<sub>3</sub> anode, *J. Hazard. Mater.*, 146 (2007) 295–301.
- [13] X.B. Wu, X.Q. Yang, D.C. Wu, R.W. Fu, Feasibility study of using carbon aerogel as particle electrodes for decoloration of RBRX dye solution in a three-dimensional electrode reactor, *Chem. Eng. J.*, 138 (2008) 47–54.
- [14] Y. Xiong, C. He, H.T. Karlsson, X. Zhu, Performance of three-phase three-dimensional electrode reactor for the reduction of COD in simulated wastewater-containing phenol, *Chemosphere*, 50 (2003) 131–136.
- [15] Z.Y. Wang, J.Y. Qi, Y. Feng, K. Li, X. Li, Preparation of catalytic particle electrodes from steel slag and its performance in a three-dimensional electrochemical oxidation system, *J. Ind. Eng. Chem.*, 20 (2014) 3672–3677.
- [16] X.Y. Li, W. Zhu, C.W. Wang, L.W. Zhang, Y. Qian, F.Q. Xue, Y. Wu, The electrochemical oxidation of biologically treated citric acid wastewater in a continuous-flow three-dimensional electrode reactor (CTDER), *Chem. Eng. J.*, 232 (2013) 495–502.
- [17] J. Zhao, S. Ye, Y.Y. Wang, X.Y. You, L.Y. Chai, Y.D. Shu, Electrochemical degradation of acidified reed pulp black liquor with three-dimensional electrode reactor, *J. Cent. South Univ.*, 22 (2015) 2945–2953.
- [18] S.S. Mahmoud, M.M. Ahmed, Electrocatalytic oxidation of phenol using Ni–Al<sub>2</sub>O<sub>3</sub> composite-coating electrodes, *J. Alloys Compd.*, 477 (2009) 570–575.
- [19] C. Cai, H. Zhang, X. Zhong, L.W. Hou, Electrochemical enhanced heterogeneous activation of peroxydisulfate by Fe-Co/SBA-15 catalyst for the degradation of Orange II in water, *Water Res.*, 66 (2014) 473–485.
- [20] J. Ding, Q.L. Zhao, L.L. Wei, Y. Chen, X. Shu, Ammonium nitrogen removal from wastewater with a three-dimensional electrochemical oxidation system, *Water Sci. Technol.*, 68 (2013) 552–559.
- [21] S.B. Wang, Z.H. Zhu, A. Coomes, F. Haghseresht, G.Q. Lu, The physical and surface chemical characteristics of activated carbons and the adsorption of methylene blue from wastewater, *J. Colloid Interface Sci.*, 284 (2005) 440–446.
- [22] R. Berenguer, J.P. Marco-Lozar, C. Quijada, D. Cazorla-Amoros, E. Morallon, Electrochemical regeneration and porosity recovery of phenol-saturated granular activated carbon in an alkaline medium, *Carbon*, 48 (2010) 2734–2745.
- [23] J. Radjenovic, D.L. Sedlak, Challenges and opportunities for electrochemical processes as next-generation technologies for the treatment of contaminated water, *Environ. Sci. Technol.*, 49 (2015) 11292–11302.
- [24] A. Bagreev, J. Angel Menendez, I. Dukhno, Y. Tarasenko, T.J. Bandosz, Bituminous coal-based activated carbons modified with nitrogen as adsorbents of hydrogen sulfide, *Carbon*, 42 (2004) 469–476.
- [25] W.M.A.W. Daud, A.H. Houshamnd, Textural characteristics, surface chemistry and oxidation of activated carbon, *J. Nat. Gas Chem.*, 19 (2010) 267–279.
- [26] P. Chingombe, B. Saha, R.J. Wakeman, Surface modification and characterisation of a coal-based activated carbon, *Carbon*, 43 (2005) 3132–3143.
- [27] T.A. Fouladi, T. Kaghazchi, M. Soleimani, Adsorption of cadmium from aqueous solutions on sulfurized activated carbon prepared from nut shells, *J. Hazard. Mater.*, 165 (2009) 1159–1164.
- [28] E. Lorencgrabowska, G. Gryglewicz, Adsorption characteristics of Congo Red on coal-based mesoporous activated carbon, *Dyes Pigm.*, 74 (2007) 34–40.
- [29] F. Lian, C. Chang, Y. Du, L.Y. Zhu, B.S. Xing, C. Liu, Adsorptive removal of hydrophobic organic compounds by carbonaceous adsorbents: a comparative study of waste-polymer-based, coal-based activated carbon, and carbon nanotubes, *J. Environ. Sci.*, 24 (2012) 1549–1558.
- [30] W.G. Li, X.J. Gong, K. Wang, X.R. Zhang, W.B. Fan, Adsorption characteristics of arsenic from micro-polluted water by an innovative coal-based mesoporous activated carbon, *Bioresour. Technol.*, 165 (2014) 166–173.
- [31] J.B. Parsa, M. Golmirzaei, M. Abbasi, Degradation of azo dye C.I. Acid Red 18 in aqueous solution by ozone-electrolysis process, *J. Ind. Eng. Chem.*, 20 (2014) 689–694.

- [32] C. Zhang, Y.H. Jiang, Y.L. Li, Z.X. Hu, L. Zhou, M.H. Zhou, Three-dimensional electrochemical process for wastewater treatment: a general review, *Chem. Eng. J.*, 228 (2013) 455–467.
- [33] C.A. Martínez-Huitle, S. Ferro, Electrochemical oxidation of organic pollutants for the wastewater treatment: direct and indirect processes, *Chem. Soc. Rev.*, 35 (2006) 1324–1340.
- [34] G.F. Lv, D.C. Wu, R.W. Fu, Performance of carbon aerogels particle electrodes for the aqueous phase electro-catalytic oxidation of simulated phenol wastewaters, *J. Hazard. Mater.*, 165 (2009) 961–966.
- [35] L. Li, X. Fang, D. Zhang, Y. Huang, The adsorption and oxidation of ammonia in granular activated carbon packed three-dimensional electrode reactor, *Int. J. Electrochem. Sci.*, 10 (2015) 4083–4089.
- [36] C.T. Wang, W.L. Chou, Y.M. Kuo, F.L. Chang, Paired removal of color and COD from textile dyeing wastewater by simultaneous anodic and indirect cathodic oxidation, *J. Hazard. Mater.*, 169 (2009) 16–22.